Redox Biology 30 (2020) 101431

Contents lists available at ScienceDirect

Redox Biology

journal homepage: www.elsevier.com/locate/redox

Research Paper

Excessive oxidative stress in cumulus granulosa cells induced cell senescence contributes to endometriosis-associated infertility

Xiang Lin[a,b,1], Yongdong Dai[a,b,1], Xiaomei Tong[a,b], Wenzhi Xu[a,b], Qianmeng Huang[a,b], Xiaoying Jin[a,b], Chao Li[a,b], Feng Zhou[a,b], Hanjin Zhou[a,b], Xiaona Lin[a,b], Dong Huang[a,b], Songying Zhang[a,b,*]

[a] Assisted Reproduction Unit, Department of Obstetrics and Gynecology, Sir Run Run Shaw Hospital, Zhejiang University School of Medicine, No. 3 Qingchun East Road, Jianggan District, Hangzhou, 310016, China
[b] Key Laboratory of Reproductive Dysfunction Management of Zhejiang Province, No. 3 Qingchun East Road, Jianggan District, Hangzhou, 310016, China

ARTICLE INFO

Keywords:
Senescence
Endometriosis
Cumulus granulosa cell
Oxidative stress
Endoplasmic reticulum stress
Infertility

ABSTRACT

Endometriosis an important cause of female infertility and seriously impact physical and psychological health of patients. Endometriosis is now considered to be a public health problem that deserves in-depth investigation, especially the etiopathogenesis of endometriosis-associated infertility. We aimed to illuminate the etiopathogenesis of endometriosis-associated infertility that involve excessive oxidative stress (OS) induced pathological changes of ovary cumulus granulosa cell (GCs). Senescence-associated β-galactosidase (SA β-gal) activity in GCs from endometriosis patients, soluble isoform of advanced glycation end products receptor (sRAGE) expression in follicular fluid from endometriosis patients and differentially expressed senescence-associated secretory phenotype factors (IL-1β, MMP-9, KGF and FGF basic protein) are all useful indexes to evaluate oocyte retrieval number and mature oocyte number. RNA-sequencing and bioinformatics analysis indicated senescent phenotype of endometriosis GCs and aggravated endoplasmic reticulum (ER) stress in endometriosis GCs. Targeting ER stress significantly alleviated OS-induced GCs senescence as well as mitochondrial membrane potential (MMP) and adenosine triphosphate (ATP) reduction in GCs. Moreover, melatonin administration rescued OS-enhanced ER stress, cellular senescence, and MMP and ATP abnormities of endometriosis GCs *in vitro* and *in vivo*. In conclusion, our results indicated excessive reactive oxygen species induces senescence of endometriosis GCs via arouse ER stress, which finally contributes to endometriosis-associated infertility, and melatonin may represent a novel adjuvant therapy strategy for endometriosis-associated infertility.

1. Introduction

Endometriosis is a common estrogen-dependent gynecological disorder characterized by the presence of functional endometrial-type mucosa outside the uterine cavity that affects up to 50% of infertile women of reproductive age [1]. The altered follicular microenvironment in endometriosis patients is a contributing factor to infertility [2]. Oxidative stress (OS) or the imbalance between reactive oxygen species (ROS) and antioxidants in the follicular microenvironment is an important factor that induces endometriosis-associated infertility and has been speculated to negatively affect folliculogenesis, oocyte maturation, ovulation and embryogenesis [3,4]. GCs in the follicular microenvironment are in the immediate vicinity of oocytes and play a critical role in the competency of oocyte via direct gap junctions [5]. Moreover, well-orchestrated cross talk between oocytes and surrounding granulosa cells (GCs) determines oocyte competency, female fertility and outcomes of assisted reproductive therapy [2]. However, current research about the impacts of OS on GCs is inadequate and indirect.

Senescence is a stress response that occurs via a highly conserved mechanism to prevent cells from various stress-induced damage including OS, genotoxic damage and inflammation stimuli [6]. Senescent cells are characterized by irreversible cell cycle arrest and distinctive metabolic activity that generates numerous soluble factors, a phenotype termed senescence-associated secretory phenotype (SASP). SASP factor impacts adjacent cells by chronically disturbing the microenvironment in an autocrine or paracrine manner [7]. The widely accepted “free

* Corresponding author. Assisted Reproduction Unit, Department of Obstetrics and Gynecology, Sir Run Run Shaw Hospital, Zhejiang University School of Medicine, No. 3 Qingchun East Road, Jianggan District, Hangzhou, 310016, China.
E-mail address: zhangsongying@zju.edu.cn (S. Zhang).
[1] These authors contributed equally to this work.

https://doi.org/10.1016/j.redox.2020.101431
Received 12 December 2019; Received in revised form 6 January 2020; Accepted 10 January 2020
Available online 12 January 2020

radical theory" explains ageing as a consequence of oxidative damage and indicated ROS as the driving force of senescence [8,9].

Excessive ROS frequently disturbs normal redox homeostasis in the endoplasmic reticulum (ER), usually inducing ER stress, which provokes the unfolded protein response (UPR) by activating genes encoding factors involved in protein folding and antioxidative machinery to restore ER homeostasis [10]. However, during unresolved UPR, persistent ER stress and excessive OS interact and reinforce each other in a positive feedback manner [10]. Emerging evidence has shown that ROS induced ER stress determinate cell state or fate, like autophagy, apoptosis, or senescence [10,11]. In addition, overactive ER stress and accumulation of misfolded proteins occur concomitantly with senescence and participate in the onset or maintenance of senescent features [12]. Whether excessive ROS in the follicular microenvironment in endometriosis enhance GCs senescence by activating ER stress is unknown.

Although telomere attrition, oncogene activation or inactivation all have been considered as inducers of cellular senescence, excessive ROS and ER abnormal UPR are the only unremitting perturbation events that occur in the onset, aggravation, and maintenance of the senescent phenotype [12]. The most accepted theory of follicle senescence emphasize reduced ability of GCs to counteract ROS as causative factors [13], which finally result in reduced follicle number, compromised follicle quality and aberrant reproductive endocrinology in ovary [14]. Whether GCs senescence plays a role in endometriosis, which is also associated with excessive OS, is unclear.

Here we explored the etiopathogenesis of endometriosis-associated infertility that involves excessive OS-induced pathological changes in cumulus GCs. We speculated that OS drives ER stress and mitochondrial dysfunction of GCs in endometriosis and eventually induces cellular senescence and generates SASP in the follicle. Studying ROS-related mechanisms that trigger cellular senescence and clarifying pathological changes in GCs in endometriosis may help develop new strategies to improve follicle quality and pregnancy outcome.

2. Material and methods

2.1. Study approval

This study was initiated on March 3, 2016 and terminated on September 28, 2019. The study was approved and monitored by the ethics committee of Sir Run Run Shaw Hospital, Zhejiang University. Informed written consent was obtained from each patient before sample collection. Female or male ICR mice were maintained in accordance with the National Institutes of Health Guide for the Care and Use of Laboratory Animals, and the experiments were approved by the Committee of Experimental Animal Ethics, Zhejiang University.

2.2. Controlled ovarian stimulation

We enrolled a total of 258 infertile patients, including 131 patients with both laparoscopic and histological diagnosis of deeply infiltrating endometriosis and 127 controls with tubal infertility at the Sir Run Run Shaw Hospital, Zhejiang University School of Medicine. All patients were treated with identical protocols this cycle for controlled ovarian stimulation with standard gonadotrophin-releasing hormone agonist combined with human menopausal gonadotropin (hMG) protocol. Detailed inclusion and exclusion criteria and assisted reproductive treatment procedures are described in the Supplementary Information.

2.3. Human follicular fluid and GC collection

Follicular fluid (FF) was collected at the time of oocyte retrieval only from leading follicles with a diameter > 18 mm. GCs were mechanically removed by cutting the cumulus layer of each leading oocyte and washing twice in phosphate buffer saline (PBS) followed by centrifugation (800 rpm for 5 min at 4 °C). Detailed procedures are presented in the Supplementary Information. Demographics, clinical characteristics and outcomes of patients are listed in Supplementary Table 1.

2.4. Cell lines and treatments

Human GC lines KGN and COV434 were purchased from American Type Culture Collection (Rockville, MD, USA). H_2O_2 at 100 μM was used to induce oxidative stress. Cells were treated with or without 100 μM H_2O_2 for 24 h or pretreated with 100 μM melatonin for 8 h followed by 100 μM H_2O_2 for 24 h. Cells were treated with TUDCA at 1 mg/mL for 12 h before 100 μM H_2O_2 treatment for 24 h.

2.5. Flow cytometry assay of ROS

Intracellular ROS levels in GCs were examined using 2′-7′-dichlorodihydrofluorescein diacetate (DCFH-DA)-based flow cytometry according to the manufacturer's instruction (S0033, Beyotime Biotechnology, Shanghai, China). Detailed procedures are presented in the Supplementary Information.

2.6. Western blot

Western blot analyses were performed as usual procedures. Antibodies are listed in Supplementary Table 2. Detailed procedures are presented in the Supplementary Information.

2.7. SA β-gal assay

SA β-gal assay was carried out according to the manufacturer's instruction (C0602, Beyotime Biotechnology). Freshly collected GCs were seeded on 12-well plates at a density of 5×10^5 cells/ml. After 24 h, cells were washed, fixed and stained in X-gal solution overnight at 37 °C. Cells were imaged and photographed using a microscope (IX70, Olympus, Japan).

2.8. Cellular senescence quantitative assay

Senescence quantitative assay was performed in 30 control GCs and 32 GCs from endometriosis patients using the 96-well Cellular Senescence Assay Kit (CBA-231, Cell Biolabs, Inc., San Diego, CA, USA) according to the manufacturer's instruction. We lysed GCs and quantitated protein concentrations using the Pierce™ BCA Protein Assay Kit (23225, Thermo Scientific™, MA, USA) via a standard protocol. Equal amounts of protein were used to measure SA-β-gal activity. And the paired 30 control FF and 32 endometriosis FF were used for enzyme-linked immunosorbent assay.

2.9. Enzyme-linked immunosorbent assay

We analyzed 38 control FF and 34 endometriosis FF samples for soluble isoform of advanced glycation end products receptor (sRAGE) using ELISA and another paired 30 control FFs and 32 endometriosis FFs for IL-1β, GRO-β/CXCL2, FGF basic, KGF/FGF-7, HGF, MMP-9, MMP-10 and G-CSF concentration [15–17]. Detailed information and procedures are presented in the Supplementary Information.

2.10. Detection of cellular ATP levels

ATP levels in GC lysates were measured using a luminometer (Synergy H4, BioTek Instruments, Inc., USA) according to the manufacturer's instructions (S0027, Beyotime Biotechnology). Total protein was extracted from GCs samples for normalization before ATP assay.

2.11. Flow cytometry assay of MMP

MMP in fresh collected GCs was detected using the JC-1 Assay Kit (C2006, Beyotime Biotechnology) combined with flow cytometry as described in the product manual. Relative MMP ratio was calculated as red fluorescence intensity/green fluorescence intensity. Cells without JC-1 staining were used as a negative control, and cells incubated with CCCP (10 μM) for 30 min were used as the positive control. The relative signal intensities of JC-1 aggregates and monomers were normalized to the control group.

2.12. Transmission electron microscopy

We examined 6 Control GCs and 6 endometriosis GCs samples, and 200 mitochondria were evaluated in at least 5 random sections for each sample; the average abnormal mitochondria rate in each group was calculated [18]. Detailed information and procedures are presented in the Supplementary Information.

2.13. RNA-seq and bioinformatics analysis

High throughput sequencing and bioinformatics analyses were conducted at RiboBio (Guangzhou, China). We first performed RNA-seq to compare the global gene expression profile between control GCs (n = 4) and endometriosis GCs (n = 5). PCA was then conducted. Volcano plot of differentially expressed mRNAs (DEMs) was generated using the gplots package in Bioconductor. DEMs with log2 (Fold Change) > 1 were labeled in red ($P < 0.05$); DEMs with log2 (Fold Change) < -1 were marked in green ($P < 0.05$). Only transcripts with more than two-fold change and a corrected P value less than 0.05 were considered statistically significant.

2.14. Gene set enrichment analysis (GSEA)

Because no gene set is available for SASP, we first pre-defined a SASP gene set based on various published microarray or sequencing analysis [15,16]. The detailed SASP gene set list is presented in Supplementary Table 3. Based on KEGG biological pathway database (http://www.genome.jp/kegg/) or Gene Ontology Consortium database (http://www.geneontology.org/), we performed GSEA (using GSEA 3.0, http://www.broadinstitute.org/gsea/) to explore the expression of gene sets related to OS, antioxidant metabolism, cell aging, cellular senescence, SASP, ER stress and UPR in control GCs and endometriosis GCs.

2.15. Establishment of the endometriotic mouse model

A total of 84 ICR mice (including 12 donors) were included in our study. A total of 24 endometriosis model mice were surgery-induced by mouse-mouse intraperitoneal implantation as described previously [19], with modifications. Detailed information and procedures are presented in the Supplementary Information and Supplementary Fig. 1.

2.16. Immunohistochemistry

Mice from each of the treatment groups (n = 6 per group) were examined. After four weeks, each mouse was intraperitoneally injected with pregnant mare serum gonadotropin (110914564, Sanshengsheng Biotechnology Co., LTD, Ningbo, China) for 48 h followed by chorionic gonadotrophin for 12–14 h before euthanasia. Ovaries were removed for immunohistochemistry. The endometriotic cysts were also excised and the volumes of endometriotic cysts were calculated as follows: V (volume) = LW2/2, in which L represents the largest length and W represents the smallest width. Antibodies are listed in Supplementary Table 2 and detailed procedures are presented in the Supplementary Information.

2.17. Fertility assessment

Fourteen days after treatment, mice from each of the groups (n = 6 for each group) in estrus were separated and housed with fertile male mice (1:1) at the same day (re-defined as day 0). Vaginal plug was checked to confirm mating on the days after mating, and all female mice were used for recording births. Pup sizes were determined at 21 days after birth (the day of weaning). The fertility test proceeded over six months and detailed procedures are presented in Supplementary Fig. 1.

2.18. Statistical analysis

All experiments were conducted at least in triplicate. SPSS program version 19.0, Graph Pad Prism 5 software was used for statistical analysis. Statistical comparison between two groups was carried out using the unpaired Student's t-test after confirming the normal distribution of the data by One-Sample Kolmogorov-Smirnov Test or Mann-Whitney U Test. The comparison of continuous variables among groups was carried out by one-way ANOVA followed by LSD tests. Pearson correlation analysis was used to estimate the correlation between different clinical outcomes and independent variables of SA β-gal expression in GCs, sRAGE in FF or SASP factors expression based SASP score. $P < 0.05$ was considered statistically significant.

3. Results

3.1. Cumulus GCs from endometriosis patients show increased ROS and excessive OS

We first examined ROS levels in fresh collected *in vitro* fertilization (IVF) patient GCs by flow cytometry and found significantly increased intracellular ROS in GCs from endometriosis patients compared with control GCs (Fig. 1A, Fig. 1B; $P < 0.001$). Excessive ROS accumulation in endometriosis GCs was also demonstrated at the protein level, as anti-oxidases inducible nitric oxide synthase (iNOS) and superoxide dismutase 1 (SOD1) were significantly reduced in these GCs compared with control GCs (Fig. 1C, Supplementary Fig. 2A; $P < 0.05$).

3.2. Cumulus GCs in endometriosis patients show senescence phenotype

Free radical accumulation or free radical theory extended mitochondria defect associated OS is the most common inducer of cellular senescence [20,21]. Moreover, DNA damage is a hallmark of OS-induced cell senescence [22]. We examined the expressions of DNA damage-associated proteins (p-BRCA1, p-ATM and p-CHK2) in human GCs and found that all proteins were notably increased in endometriosis GCs compared with control GCs (Fig. 1C, Supplementary Fig. 2A; $P < 0.05$). These results suggested that GCs in endometriosis may undergo OS-induced DNA damage-associated senescence.

Senescence-associated β-galactosidase (SA β-gal) assays revealed increased SA β-gal activity in endometriosis GCs compared with control GCs (Fig. 1D and E; $P < 0.001$). We also observed a negative correlation between SA β-gal activity of GCs from endometriosis patients and patient oocyte retrieval number and mature oocyte number by linear regression analysis (Fig. 1F, R = 0.611 for oocyte retrieval number and R = 0.646 for mature oocyte number, both $P < 0.001$).

Cell cycle arrest is an important characteristic of senescent cells [6,7]. We found that the percentage of GCs in G1 phase was significantly increased in the endometriosis group compared with controls (Supplementary Fig. 2B, Supplementary Fig. 2C; $P < 0.01$).

Soluble isoform of advanced glycation end products receptor (sRAGE) is a useful parameter of GC senescence that shows a protective function in follicular fluid via binding to oxidative ligands and interrupts advanced glycation end products receptor (RAGE)-mediated pathological conditions or intracellular signaling [23,24]. sRAGE

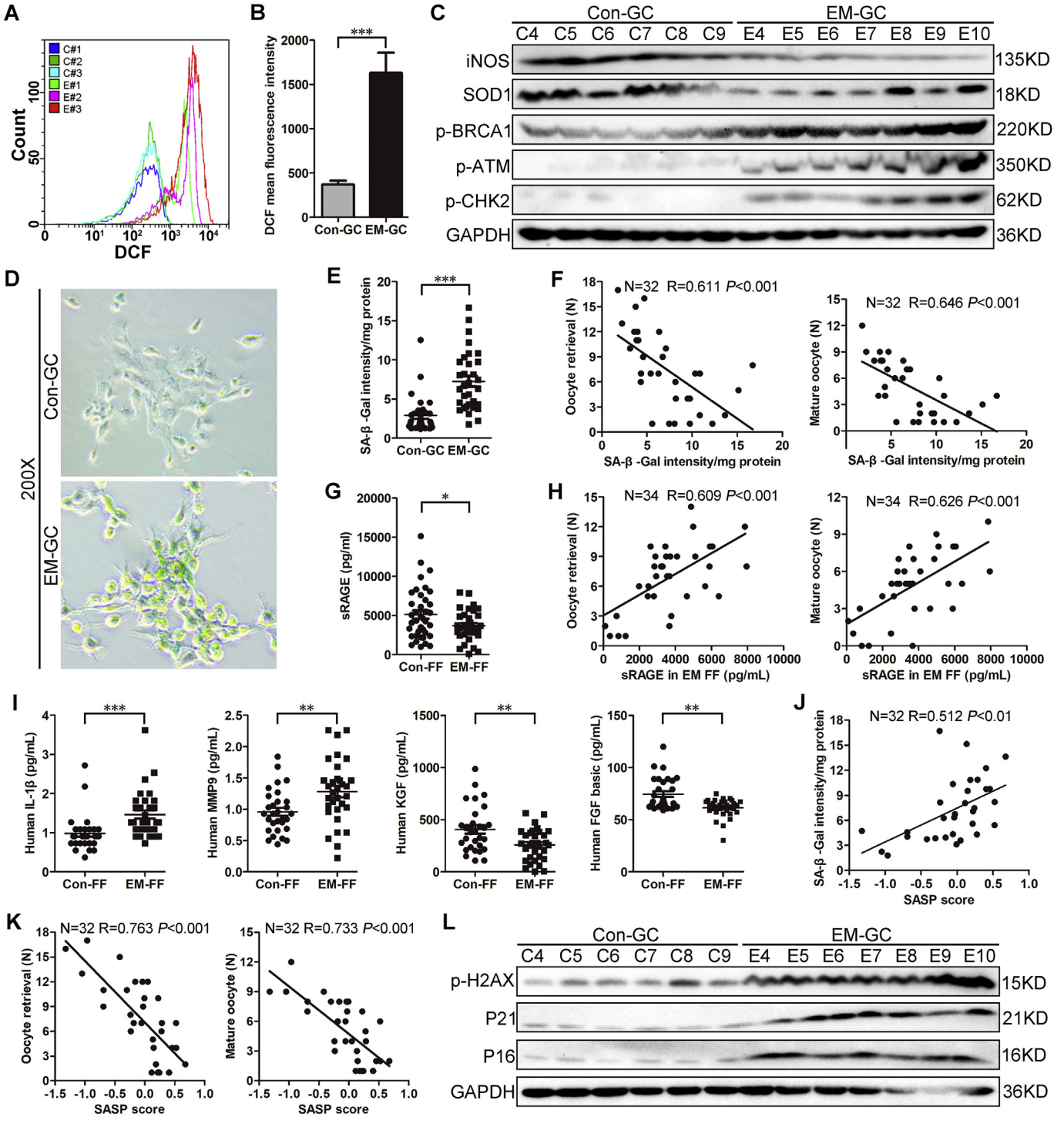

(caption on next page)

expression was significantly decreased in FF from endometriosis patients compared with FF from controls (Fig. 1G, $P < 0.05$). Linear regression analysis showed positive correlations between sRAGE levels in endometriosis FF and endometriosis patient oocyte retrieval number and mature oocyte number (Fig. 1H, R = 0.609 for oocyte retrieval number and R = 0.626 for mature oocyte number, both $P < 0.001$).

Our above results indicated that cumulus GCs in endometriosis patients show OS-induced senescence phenotype. Moreover, SA β-gal activity in endometriosis GCs and sRAGE levels in endometriosis FF are valuable parameters for indicating oocyte retrieval number and mature oocyte number in endometriosis.

3.3. Endometriosis patients show accumulated SASP factors in FF and increased senescence-associated protein expression in GCs

To more closely examine cumulus GC senescence in endometriosis, we investigated representative SASP soluble factors in FF from IVF patients using enzyme-linked immunosorbent assay. Although G-CSF, HGF, CXCL2, and MMP-10 concentrations showed no difference between endometriosis FF and control FF (Supplementary Fig. 2D), IL-1β and MMP-9 levels were significantly increased in endometriosis FF compared with control FF (Fig. 1I, $P < 0.001$), while KGF and FGF basic protein expression were significantly decreased (Fig. 1I,

Fig. 1. GCs from endometriosis patients show excessive oxidative stress and senescence.
A. Flow cytometry of intracellular ROS levels using 2′-7′-dichlorodihydrofluorescein (DCF) in control and endometriosis GCs. The colored curves represent six samples from the control (C#1, C#2, C#3) and endometriosis groups (E#1, E#2, E#3). **B.** Quantitative analysis of intracellular ROS levels via flow cytometry (n = 12 for control GCs, n = 16 for endometriosis GCs); ***$P < 0.001$, Mann-Whitney U. **C.** Western blot of indicated proteins in GCs from control and endometriosis patients (n = 6 for control GCs, n = 7 for endometriosis GCs). **D.** SA β-gal assay of control GCs (top) and endometriosis GCs (bottom) (n = 5 for control GCs, n = 5 for endometriosis GCs). Magnification, 200X. **E.** SA β-gal quantitative assay results of 30 control GCs and 32 endometriosis GCs. ***$P < 0.001$, Mann-Whitney U. **F.** Scatter diagram showing linear regression and significant Pearson correlation of oocyte retrieval number and mature oocyte number with SA β-gal activity in endometriosis GCs based on fluorescence quantitative results (n = 32); the left panel shows the correlation between oocyte retrieval number and SA β-gal activity, the right panel displays the correlation between mature oocyte number and SA β-gal activity; both $P < 0.001$. **G.** ELISA of sRAGE in human follicular fluid (n = 38 for controls, n = 34 for endometriosis patients); *$P < 0.05$, Student's t-test. **H.** Scatter diagram showing linear regression and significant Pearson correlation of oocyte retrieval number and mature oocyte number with sRAGE in endometriosis FF based on ELISA (n = 34); the left panel shows the correlation between oocyte retrieval number and sRAGE, the right panel displays the correlation between mature oocyte number and sRAGE; both $P < 0.001$. **I.** ELISA of IL-1β, MMP-9, KGF and FGF basic protein in FF (n = 30 for controls, n = 32 for endometriosis patients); ***$P < 0.001$, Mann-Whitney U; **$P < 0.01$, Student's t-test; **$P < 0.01$, Mann-Whitney U; **$P < 0.01$, Mann-Whitney U from left panel to right panel, respectively. **J.** SASP score was defined as the arithmetic sum of cumulative distribution probability of four differentially expressed SASP factors. Scatter diagram shows linear regression and significant Pearson correlation of SA β-gal activity with SASP score based on ELISA results of four differentially expressed SASP factors (n = 32 for endometriosis patients); $P < 0.01$. **K.** Scatter diagram shows linear regression and significant Pearson correlation of oocyte retrieval number and mature oocyte number with SASP score results (n = 32 for endometriosis patients); the left panel shows the correlation between oocyte retrieval number and SASP score, the right panel displays the correlation between mature oocyte number and SASP score; both $P < 0.001$. **L.** Western blot of indicated proteins in GCs from control and endometriosis patients (n = 6 for control GCs, n = 7 for endometriosis GCs). GC, granulosa cell; Con, control group; EM, endometriosis group.

$P < 0.01$). The trends of IL-1β, MMP-9, KGF and FGF basic protein in endometriosis FF were consistent with previously reported senescent cell SASP factors [15–17].

To identify the overall effects of differentially expressed SASP factors on follicle quality, we established a standardization and normalization model. Cumulative distribution function (CDF) is the probability that a corresponding continuous random variable has a value less than or equal to the argument of the function. CDF was calculated using NORMDIST (x, mu, sigma, TRUE) function in Microsoft Excel to standardize human IL-1β, MMP-9, KGF and FGF basic protein expression. SASP score was calculated as CDF (IL-1β) + CDF (MMP)-CDF (KGF)-CDF (FGF basic). Notably, a positive correlation was observed between SASP score and SA β-gal activity in GCs from endometriosis patients (Fig. 1J, R = 0.512, $P < 0.01$), while correlations between SASP score and oocyte retrieval number and mature oocyte number were negative by linear regression analysis (R = 0.763 and 0.733, respectively) (Fig. 1K, $P < 0.001$). These data demonstrated that GCs in endometriosis patients showed an abnormal SASP portfolio, and the SASP portfolio score negatively predicted the oocyte retrieval number and mature oocyte number of endometriosis patients.

Stress-associated senescence is characterized by accumulated expression of $p16^{INK4a}$, $p21^{CIPI/WAF1}$ and p-H2AX [22,25]. Western blot revealed increased p16, p21, and p-H2AX levels in endometriosis GCs, indicating increased senescence (Fig. 1L, Supplementary Fig. 2E; $P < 0.01$).

3.4. Endometriosis GCs show decreased mitochondrial transmembrane potential (MMP), reduced ATP and increased abnormal mitochondria ratio

Excessive OS is thought to hamper mitochondria function and lead to MMP reduction and energetic crisis, accompanied by cellular senescence [26]. Moreover, mitochondrial dysfunction-associated loss of MMP and ATP supply are frequently detected in aging GCs [2,18]. We thus examined MMP in GCs using JC-1 staining and flow cytometry. Immunofluorescence showed stronger green JC-1 monomer signal in endometriosis GCs than in control GCs, while the red fluorescence intensity in the endometriosis group was weaker (Fig. 2A). Flow cytometry showed increased JC-1 monomer signal and decreased JC-1 aggregate signal in endometriosis GCs compared with control GCs (Fig. 2B). Quantitative results from FCM confirmed that the relative MMP ratio was significantly decreased in endometriosis GCs compared with control GCs (Fig. 2C, $P < 0.001$). The reduced ATP levels in fresh collected GCs from endometriosis patients compared with control GCs indicated mitochondria dysfunction and energetic crisis in endometriosis GCs (Fig. 2D, $P < 0.05$).

Transmission electron microscopy revealed strikingly increased numbers of mitochondria with structural abnormalities in endometriosis GCs compared with control GCs (Fig. 2E). The proportion of abnormal mitochondria in GCs samples from 6 control patients and 6 endometriosis patients was 5.17% and 13.33%, respectively (Fig. 2F, $P < 0.01$).

3.5. Cumulus GCs from endometriosis patients show OS and senescence as well as ER stress and impaired UPR

To further explore the pathologic changes of GCs in endometriosis, we conducted RNA sequencing (RNA-seq) and combined gene-set enrichment analysis (GSEA) in GCs samples from four control patients or GCs samples from five endometriosis patients. RNA-seq normalized data were subjected to principal component analysis (PCA) by an unsupervised method to explore the variance in the mRNA dataset; PC1 and PC2 visually separated endometriosis GCs and control GCs as two distinctive clusters (Fig. 3A). We found that 411 genes were significantly up-regulated and 282 genes were significantly down-regulated in GCs from endometriosis patients compared with control GCs (fold change > 2, corrected P value < 0.05) (Fig. 3B and C).

GSEA results displayed that functional genes from “cellular response to oxidative stress” was abundantly enriched in endometriosis GCs, while antioxidative genes from the “glutathione metabolism” set were just enriched in control GCs (Fig. 3D with normalized enrichment score NES = 1.400, $P < 0.05$; Fig. 4E with NES = −1.189, $P < 0.05$), consistent with our previous results. Additionally, “regulation of cell aging,” “cell aging,” “cellular senescence” and “SASP” gene sets were enriched in endometriosis GCs (Fig. 3F with NES = 1.237, 1.195, 1.208, and 1.550, respectively, $P < 0.05$), which also confirmed the senescent phenotype of endometriosis GCs.

GCs function maintenance requires ER correctly regulate protein synthesis, folding, maturation or destroy unfolded/misfolded proteins [27]. Oxidative burden linked to ER dysfunction and accumulation of misfolded proteins [12] and senescent cells often show perturbed ER proteostasis [28]. GSEA results revealed “endoplasmic reticulum calcium ion homeostasis,” “ER associated ubiquitin dependent protein catabolic process,” “ERAD pathway,” and “IRE1 mediated unfolded protein response” function genes as enriched in endometriosis GCs with NES = 1.195, 1.390, 1.438, and 1.435, respectively (Fig. 3G, $P < 0.05$). These results revealed that OS and cellular senescence as well as ER stress and UPR were enriched in endometriosis GCs.

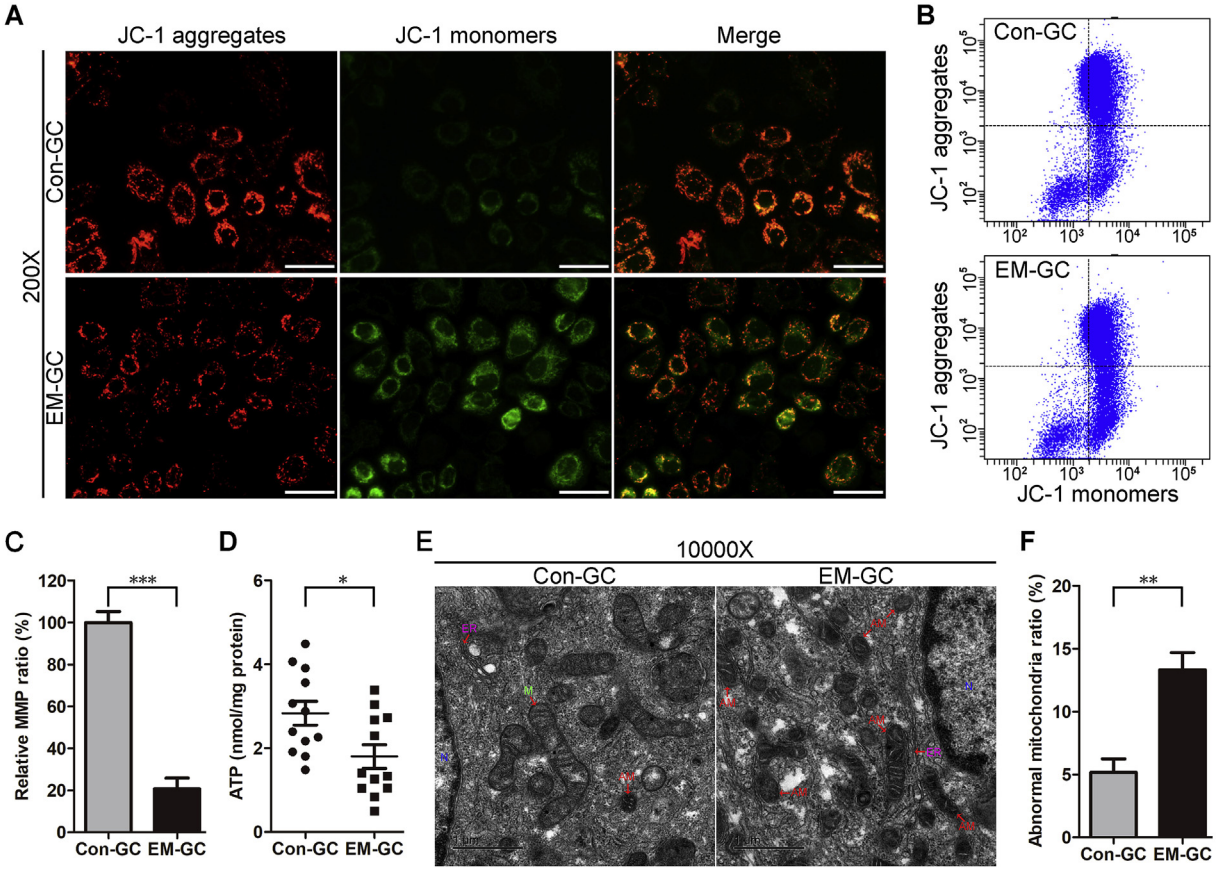

Fig. 2. Decreased mitochondrial transmembrane potential (MMP), reduced ATP levels and increased dysfunction mitochondria ratio in GCs from endometriosis patients.

A. JC-1-based immunofluorescence assay of human GCs (n = 3 for control GCs, n = 3 for endometriosis GCs); red represents JC-1 aggregate signal; green represents JC-1 monomer signal; representative image of GCs from one control and one endometriosis patient is shown; original magnification: 200X. **B.** JC-1-based flow cytometry assay of human GCs (n = 6 for control GCs, n = 9 for endometriosis GCs); images shows typical fluorescence intensity distribution of one control GC (top) and one endometriosis GC (bottom). **C.** Flow cytometry quantitative assay of MMP ratio (n = 6 for control GCs, n = 9 for endometriosis GCs); ***P < 0.001, Mann-Whitney U. **D.** Intracellular ATP levels assay in GCs (n = 12 for control GCs, n = 12 for endometriosis GCs); *P < 0.001, Student's t-test. **E.** Ultrastructure of GCs by transmission electron microscopy; original magnification: ×1000; M, normal mitochondria; AM, abnormal mitochondria; ER, endoplasmic reticulum; N, nucleus. **F.** Abnormal mitochondria proportion in 6 control GCs and 6 endometriosis GCs; for each GC sample, two individuals counted a total of 200 mitochondria in at least five random sections independently and the rate of abnormal mitochondria was recorded. The abnormal mitochondria ratio in GCs from endometriosis patients was 13.33 ± 3.33, which was significantly higher than control GCs (5.17 ± 2.64); **P < 0.01, Mann-Whitney U. . (For interpretation of the references to color in this figure legend, the reader is referred to the Web version of this article.)

3.6. OS aggravates cell senescence and induced ER stress in GC lines

ER stress results in upregulation of heat shock 70 kDa protein 5 (HSPA5 or GRP78), phosphorylated inositol-requiring enzyme 1 (p-IRE1), UPR transcription factor C/EBP homologous protein (CHOP), spliced form of X-box-binding protein 1 [XBP1(S)], activating transcription factor 4 (ATF4) and activating transcription factor 6 (ATF6) [29]. GSEA results showed accumulation of misfolded proteins in endometriosis GCs, relative expression of several ER stress-associated genes based on RNA-seq reads implied a tendency for upregulated GRP78 and IRE1 in endometriosis GCs, though a statistical difference was only observed with IRE1 gene expression (Fig. 4A; $P < 0.05$). Western blot showed that the ER stress chaperone (GRP78) and UPR activators (p-IRE1 and CHOP) were significantly increased in endometriosis GCs compared with control GCs (Fig. 4B, Supplementary Fig. 2F; $P < 0.05$), consistent with RNA-seq and GSEA results.

To clarify whether OS-induced cellular senescence is involved ER stress in GCs *in vitro*, we used H_2O_2 to generate ROS in GC lines KGN and COV434. Western blot revealed increased p16, p21, and p-H2AX protein expression and upregulated GRP78, p-IRE1 and CHOP protein levels in GC cells treated with H_2O_2 (Fig. 4C, Supplementary Fig. 2G; $P < 0.05$). Moreover, increased SA β-gal activity was observed after H_2O_2 treatment compared with controls, indicating ROS effectively induced GCs senescence and caused ER stress *in vitro* (Fig. 4D).

3.7. ER stress inhibitor protects GCs from OS-induced senescence, MMP reduction and ATP crisis

As mentioned above, senescent GCs in endometriosis may derive from mitochondrial or ER dysfunction as consequences of OS. To investigate whether reduction of ER stress could attenuate OS-induced cellular senescence in GC lines, we used the ER stress inhibitor tauro ursodesoxy cholic acid (TUDCA). Pretreatment with TUDCA for 12 h significantly rescued H_2O_2-induced SA β-gal activity increase in GC lines (Fig. 4D). While H_2O_2 treatment decreased ATP levels (Fig. 4E, $P < 0.05$), TUDCA pretreatment partly rescued ATP levels (Fig. 4E, $P < 0.05$). Furthermore, while immunofluorescence showed stronger green JC-1 monomer signal and weaker red JC-1 aggregate fluorescence in H_2O_2 group compared with control group, TUDCA pretreatment decreased green JC-1 monomer signal compared with H_2O_2 group (Fig. 4F). H_2O_2 treatment reduced the relative MMP ratio compared with controls ((Fig. 4G, $P < 0.05$), while the relative MMP ratio was significantly increased after TUDCA pretreatment compared with H_2O_2 treatment (Fig. 4G, $P < 0.05$). TUDCA pretreatment rescued ER stress-

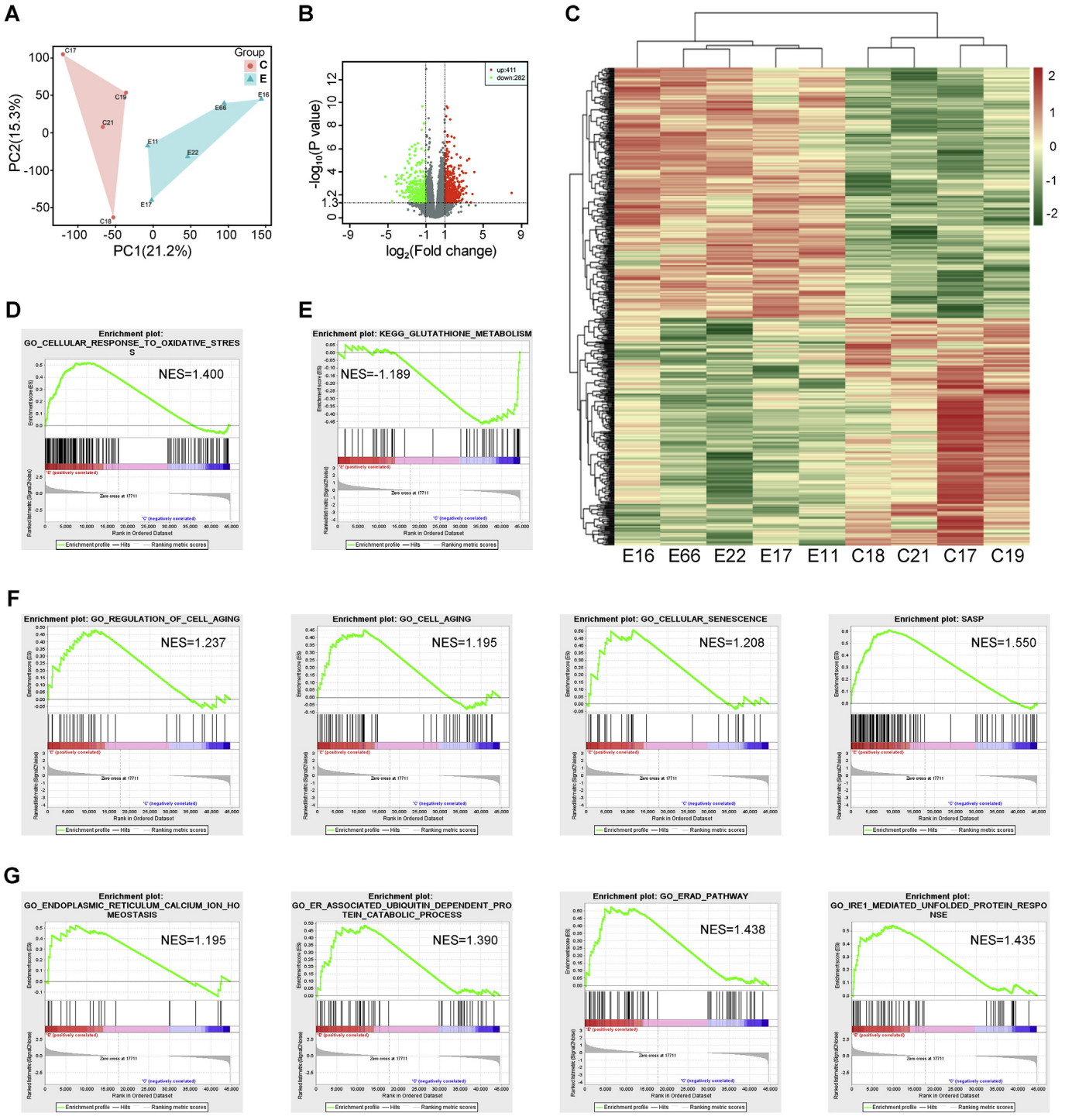

Fig. 3. Bioinformatic analysis results support oxidative stress-induced senescence of endometriosis GCs that involves increased ER stress.
A. Principal component analysis (PCA) of mRNA dataset from 4 control GCs and 5 endometriosis GCs. **B.** Differentially expressed mRNAs (DEMs) were identified using the gplots package in Bioconductor. Red and green points indicate upregulated and downregulated DEMs, respectively (fold change $>$ 2 and corrected P value $<$ 0.05). **C.** Heat map of the differentially expressed 411 up-regulated and 284 down-regulated genes. Gene set enrichment analysis (GSEA) was used to explore significantly enriched gene sets comparing the entire gene transcripts in GCs from endometriosis patients and control GCs to gene sets in GSEA Molecular Signatures Database (MsigDB); genes with expression levels closely associated with endometriosis (E) or control (C) group are located at the left or right edge of the list, respectively; Y-axis of enrichment plot, value of the ranking metric; X-axis of enrichment plot, the rank for all genes. Bottom: plot of the ranked list of all genes; the peak score of the enrichment plot represents the enrichment score (ES) for this gene set. **D.** Genes in endometriosis GCs were significantly enriched in the "cellular response to oxidative stress" gene set. **E.** Control GCs showed enhanced genes in the antioxidative "glutathione metabolism" pathway. **F.** GSEA revealed enrichment of endometriosis genes in "regulation of cell aging," "cell aging," "cellular senescence" and "SASP." **G.** Genes of "endoplasmic reticulum calcium ion homeostasis," "ER associated ubiquitin dependent protein catabolic process," "ERAD pathway," and "IRE1 mediated unfolded protein response" pathways were also enriched in GCs from endometriosis patients. NES, normalized enrichment score; false discovery rate (FDR) of all sets were less than 25%. . (For interpretation of the references to color in this figure legend, the reader is referred to the Web version of this article.)

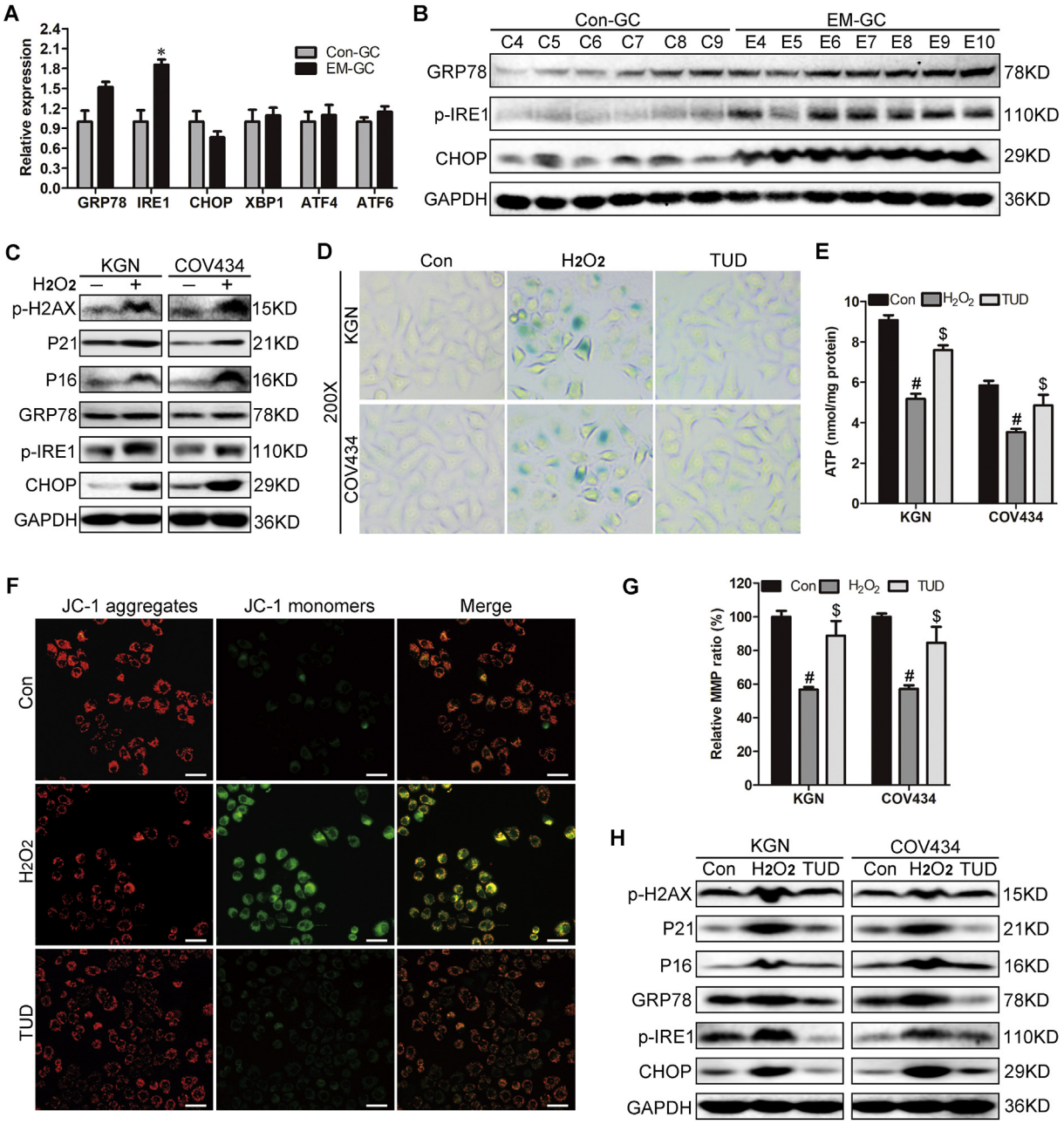

Fig. 4. Activated ER stress in GCs from endometriosis patients and anti-aging effects of TUDCA *in vitro*

A. Relative expression of ER stress-associated genes based on RNA sequencing results (n = 4 for control GCs, n = 5 for endometriosis GCs); *$P < 0.05$, Mann-Whitney U. **B.** Western blot of ER stress chaperone (GRP78) and UPR activators (p-IRE1 and CHOP) in 6 control GCs and 7 endometriosis GCs. **C.** Western blot of indicated proteins in KGN (left panel) and COV434 cells (right panel) treated with 100 μM H_2O_2 for 24 h. **D.** SA β-gal activity in KGN and COV434 cells in control, H_2O_2 and TUDCA groups (Con, H_2O_2 and TUD, respectively). Top panel shows SA β-gal staining of KGN cells and bottom shows staining of COV434 cells. Original magnification, 200X. **E.** Intracellular ATP levels in KGN and COV434 cells treated with H_2O_2 or TUDCA; #$P < 0.05$, H_2O_2 vs. Con group, one-way ANOVA with LSD for multiple comparisons; \$$P < 0.05$, TUD vs. H_2O_2 group, one-way ANOVA with LSD for multiple comparisons. **F.** JC-1-based immunofluorescence of KGN and COV434 cells from control, H_2O_2 and TUDCA groups. Representative images of each group are shown; original magnification: 200×. **G.** MMP ratio in KGN and COV434 cells from control, H_2O_2 and TUDCA groups; #$P < 0.05$, H_2O_2 vs. Con group, one-way ANOVA with LSD for multiple comparisons; \$$P < 0.05$, TUD vs. H_2O_2 group, one-way ANOVA with LSD for multiple comparisons. **H.** Western blot of indicated proteins in control, H_2O_2 and TUDCA treated KGN and COV434 cells.

associated GRP78, p-IRE1, and CHOP expressions and down-regulated p16, p21 and p-H2AX expressions compared with H_2O_2-treated cells (Fig. 4H, Supplementary Fig. 2G; $P < 0.05$). Our results suggest an ER stress-dependent mechanism in ROS-induced senescence of GCs.

3.8. Melatonin attenuates OS-induced senescence via upregulating antioxidase expression and suppressing ER stress in vitro

As ROS is the root of GCs senescence and due to the unclear reproduction toxicity of TUDCA, we investigated whether antioxidants could attenuate OS-induced ER stress and senescence in GCs. Melatonin, a stable robust antioxidant, has shown promising clinical applications in aging-related diseases and is believed to delay ovarian aging by multiple mechanisms [30]. Pretreatment with melatonin for 8 h significantly rescued the H_2O_2-induced SA β-gal activity increase in KGN and COV434 cells (Fig. 5A). Moreover, the ROS-induced reduction of ATP levels was rescued by melatonin pretreatment (Fig. 5B; both $P < 0.05$). Melatonin pretreatment significantly rescued MMP levels

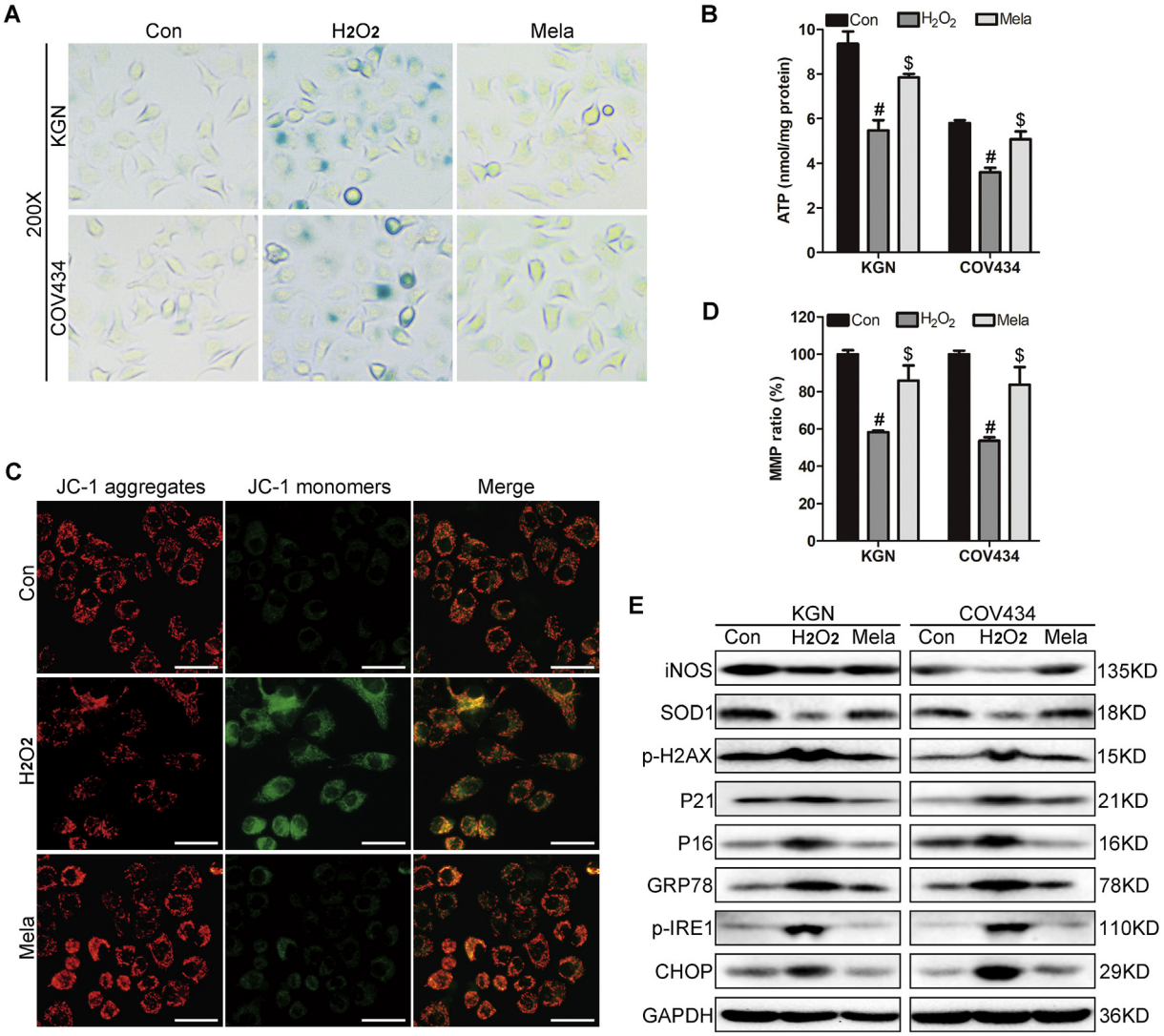

Fig. 5. ***Melatonin attenuates oxidative stress-induced senescence via suppressing ER stress in vitro***

A. SA β-gal activity of KGN and COV434 cells in control, H_2O_2 and melatonin groups. Original magnification, 200X. **B.** Intracellular ATP levels in KGN and COV434 cells treated with H_2O_2 or melatonin; $\#P < 0.05$, H_2O_2 vs. Con group, one-way ANOVA with LSD for multiple comparisons; $\$P < 0.05$, Mela vs. H_2O_2 group, one-way ANOVA with LSD for multiple comparisons. **C.** JC-1-based immunofluorescence assay of KGN and COV434 cells from control, H_2O_2 and melatonin groups; representative images are shown. Original magnification: 200X. **D.** MMP ratio in KGN and COV434 cells from control, H_2O_2 and melatonin groups; $\#P < 0.05$, H_2O_2 vs. control group, one-way ANOVA with LSD for multiple comparisons; $\$P < 0.05$, Mela vs. H_2O_2 group, one-way ANOVA with LSD for multiple comparisons. **E.** Western blot results of indicated proteins in control, H_2O_2 and melatonin treated KGN and COV434 cells. All experiments were repeated at least three times and results of representative experiments are shown.

via reducing JC-1 monomers and upregulating JC-1 aggregates (Fig. 5C). ROS-induced reduction of relative MMP ratio was significantly rescued after melatonin pretreatment (Fig. 5D; both $P < 0.05$). The anti-oxidative and anti-aging effects of melatonin were confirmed at molecular levels, as melatonin upregulated anti-oxidase iNOS and SOD1 expressions, suppressed ER stress-associated GRP78, p-IRE1, and CHOP expressions and decreased senescence-associated p16, p21 and p-H2AX expressions compared with H_2O_2 treatment group (Fig. 5E, Supplementary Fig. 2I; $P < 0.05$).

3.9. Melatonin alleviates OS-induced fertility decline via suppressing ER stress and restores GC antioxidative function in vivo

We showed that melatonin effectively suppressed ER stress and alleviated GC senescence *in vitro,* and we previously demonstrated that antioxidants effectively alleviate endometriosis progression [19]. We next explored whether melatonin recovers antioxidative function of GCs in ovaries of an endometriosis mouse model. Classical endometriosis-like lesions were successfully formed in the endometriosis mouse group (EM) and melatonin pretreatment group (EM + Mela); no ectopic adhesion lesions or inflammation were observed in the sham-operated group (Fig. 6A). Notably, endometriotic lesion sizes were significantly smaller in the EM + Mela group than in the endometriosis group (Fig. 6A and B; $P < 0.001$), although the detailed mechanism needs further research.

The flow chart of mouse experiments is shown in Supplementary Fig. 1. We next used 3-nitropropionic acid (3-NAP), an agent used in rodents to evoke and maintain high ROS levels *in vivo*, to establish an OS mouse model [31,32].

The delivery times of mice in Con, Con + Mela and 3-NAP + Mela groups were 8 within 6 months, but the delivery times of mice from 3-NAP, EM and EM + Mela groups were 7 within 6 months. Mice from Con, Con + Mela and 3-NAP + Mela groups took 21 days to produce the first pups, while mice from 3-NAP, EM and EM + Mela groups took

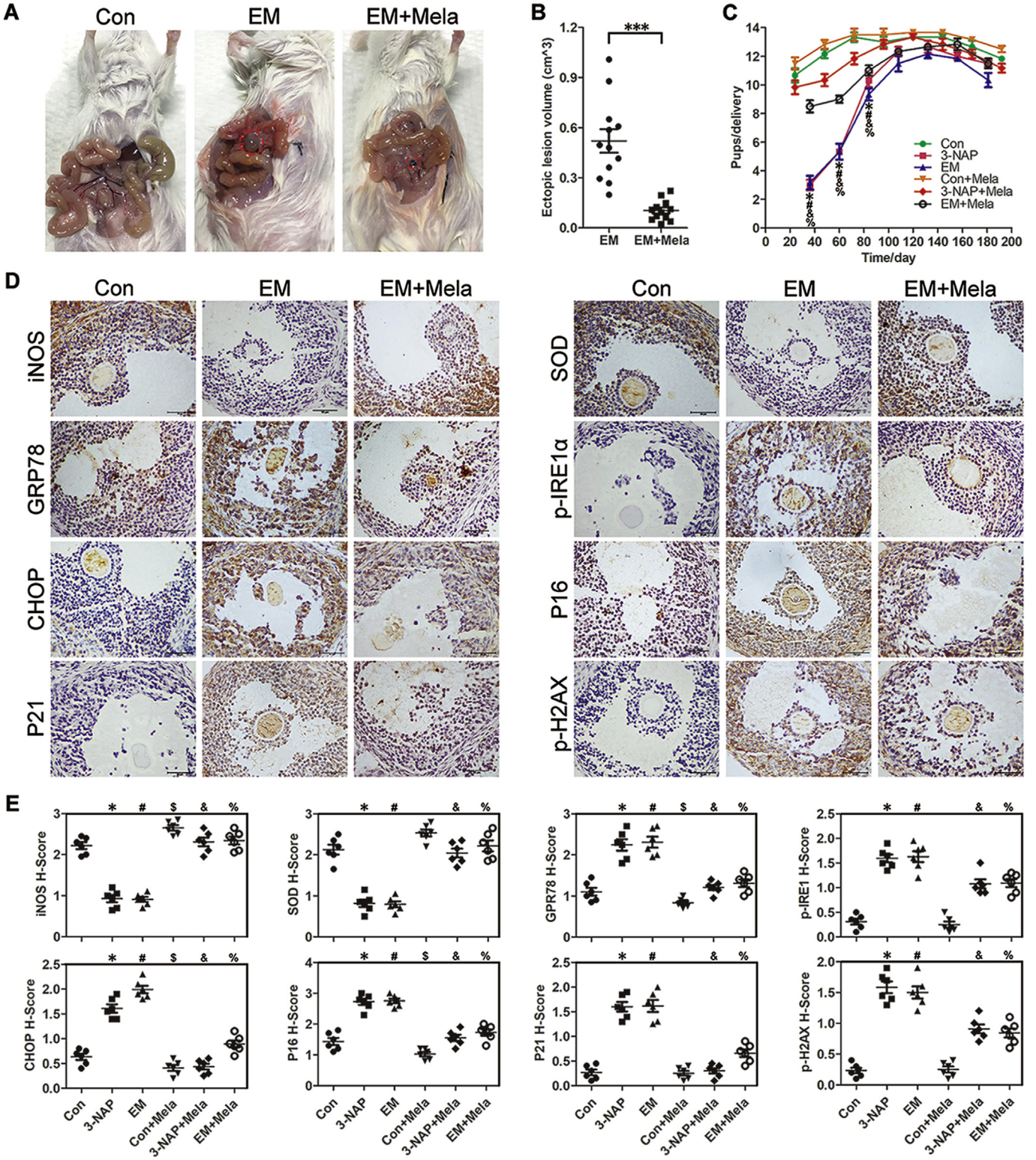

Fig. 6. Melatonin alleviates oxidative stress-induced fertility decline via suppressing ER stress and restoring GC antioxidant function in vivo

A. Representative visible endometriosis-like lesions in the peritoneal cavity of endometriosis group mice (EM) and melatonin-pretreated endometriosis mice (EM + Mela) four weeks after surgery. The first panel shows the normal peritoneal cavity of control group mice (Con). **B**. Scatter plot of lesion volumes from EM and EM + Mela mice (n = 12 for EM, n = 12 for EM + Mela mice); ***P < 0.001, Student's t-test. **C**. The development of mouse fertility within 6 months of mating. The horizontal axis shows time (days) from mating; the vertical axis indicates average pup number of each delivery (pups/delivery). **D**. Immunohistochemistry of indicated proteins in mouse ovary granulosa cells from control, endometriosis and melatonin pretreatment groups (Con, EM, EM + Mela, respectively). Each group contained 6 mice. Scale bars = 50 μm; original magnification: 400X; staining was developed using diaminobenzidine and nuclei were stained with hematoxylin. **E**. Immunohistochemistry H-score of iNOS, SOD1, GRP78, p-IRE1, CHOP, p16, p21 and p-H2AX in ovary granulosa cells from control (Con), 3-nitropropionic acid (3-NAP), endometriosis (EM), control mouse with melatonin (Con + Mela), 3-nitropropionic acid and melatonin combined treatment (3-NAP + Mela) and melatonin treated endometriosis groups (EM + Mela); n = 6 for each group; *P < 0.05, 3-NAP vs. Con; #P < 0.05, EM vs. Con; $P < 0.05, Con + Mela vs. Con; &P < 0.05, 3-NAP + Mela vs. 3-NAP; %P < 0.05, EM + Mela vs. EM; all one-way ANOVA with LSD for multiple comparisons. H-Score of different proteins shown on the vertical axis and six groups indicated on the horizontal axis.

30 days (Fig. 6C, $P < 0.05$ vs. control group), though no significant delay of production was observed after the first delivery between groups. The average number of offspring over a 6 month period was significantly decreased in 3-NAP and EM groups compared with the Con group (Supplementary Fig. 2J, both $P < 0.05$ vs. Con), while the average number of pups within 6 months in groups treated with melatonin (Con + Mela, 3-NAP + Mela and EM + Mela groups) was significantly increased compared with paired non-melatonin groups (Con, 3-NAP or EM groups) (Supplementary Fig. 2J, all $P < 0.05$).

During the first 3 month period after pairing, the average pup number in each delivery was significantly lower in the 3-NAP and EM groups than in the Con group (Fig. 6C, both $P < 0.05$ vs. Con); the increased pup number per delivery in Con + Mela group compared with Con group did not reach significant difference. Moreover, in the first three months, the average pup number of each delivery in the 3-NAP + Mela and EM + Mela groups was significantly larger than in the paired 3-NAP and EM groups (Fig. 6C; both $P < 0.05$), but no statistic difference was found in the number of pups between paired groups (Con vs. 3-NAP, Con vs. EM, Con vs. Con + Mela, 3-NAP vs. 3-NAP + Mela, EM vs. EM + Mela) after 3 months of mating. No significant fluctuations were detected in average pup weight at the time of weaning (Supplementary Fig. 2K).

Immunohistochemistry showed that iNOS and SOD1 expressions in mouse ovary GCs in endometriosis group were decreased compared with controls, while GRP78, p-IRE1, CHOP, p16, p21 and p-H2AX expressions were increased (Fig. 6D and E; $P < 0.05$ EM vs. control group). Melatonin-treated EM mice showed increased iNOS and SOD1 expressions and decreased GRP78, p-IRE1, CHOP, p16, p21 and p-H2AX expressions compared with the EM group (Fig. 6D and E; $P < 0.05$). Mouse ovary GCs from the 3-NAP group showed weak iNOS and SOD1 expression, but positive GRP78, p-IRE1, CHOP, p16, p21 and p-H2AX expressions (Fig. 6E; $P < 0.05$, 3-NAP vs. Con), indicating that ROS resulted in ER stress and finally induced senescence of GCs *in vivo*. Notably, melatonin significantly rescued 3-NAP-induced iNOS and SOD1 reduction and decreased ROS-generated GRP78, p-IRE1, CHOP, p16, p21 and p-H2AX expressions (Fig. 6E, $P < 0.05$, 3-NAP + Mela vs. 3-NAP). In the sham-operated group, melatonin significantly increased mouse GC iNOS expression compared with control group and slightly decreased GRP78, CHOP and p16 expressions, though no significant differences were found in SOD1, p-IRE1, p21 and p-H2AX expressions (Fig. 6E, $P < 0.05$, Con + Mela vs. Con). These data indicate that melatonin can delay senescence of GCs in endometriosis and reduce endometriosis-associated fertility decline via suppressing ER stress *in vivo*.

4. Discussion

Oxidative damage results in compromised follicles in endometriosis linked to fecundity decreases [3,4], though the detailed mechanism is unclear. Here we provide direct evidence of excessive ROS in endometriosis GCs and revealed ROS induced GCs senescence eventually contributed to endometriosis-associated infertility. Moreover, ROS induced GCs senescence via activating ER stress and harm mitochondria function, and senescence associated SA β-gal activity in endometriosis GCs, sRAGE expression in endometriosis FF and differentially expressed SASP factors based SASP score in endometriosis are all significant correlated with oocyte retrieval number and mature oocyte number of endometriosis patient.

It's the first time that GC senescence has been concerned and proved in endometriosis-associated infertility. Previous studies considered GC apoptosis as an important reason of compromised follicle quality and adverse ART results in endometriosis [33]. However, no studies examined the aberrant senescence-associated secretory phenotype in endometriosis FF. Increased AGE/sRAGE ratio in FF was recently reported as associated with activation of the UPR in GCs and led to decreased oocyte developmental competence [34], consistent with our results.

To date, no evidence has demonstrated telomere shortening in endometriosis GCs and robust telomerase has been detected in endometriosis endometrium and ectopic lesions [35], as well as greater telomere content in peripheral blood from endometriosis patients [36]. Our results revealed excessive OS and DNA damage in GCs from endometriosis patients, which led us to speculate that OS induced senescence of GCs in endometriosis. Additionally, the reduced iNOS and SOD1 levels in endometriosis GCs, the defective mitochondrial function of endometriosis GCs, and the accumulation of sRAGE in endometriosis FF were consistent with pathologic changes of GCs from older women (over 38 years) who suffer from OS injury [2,18,37].

Activation of ER stress in GCs leads to impaired cumulus-oocyte complex maturation, follicle apoptosis, follicle metabolic disturbance or ovarian fibrosis [29,38,39]. We found significantly increased ER stress marker expression and decreased MMP ratio and ATP production in GCs from endometriosis patients. As the ER stress inhibitor efficiently protected GCs from H_2O_2-induced senescence and mitochondrial dysfunction *in vitro*, we suspected an ER stress-dependent mechanism of GCs senescence in endometriosis, although we cannot completely rule out that it may be a concomitant event.

The ER stress inhibitor TUDCA is a taurine conjugate of ursodeoxycholic acid that is mostly used for cholestatic liver diseases. However, due to its cumulative toxicity and unknown risk of damage in reproductive system, we chose the safer antioxidant melatonin to explore potential clinical treatment of endometriosis. Melatonin, a pleiotropic endogenous hormone produced by the pineal gland, effectively reduces OS under multiple circumstances by a direct free radical scavenging mechanism or by indirectly upregulating antioxidant enzymes [40]. Melatonin exerts protective functions against aging-induced fertility decline by preserving mitochondrial cardiolipin integrity, enhancing mitochondrial antioxidant activities and maintaining mitochondrial redox balance [41,42]. In addition, melatonin not only improved mouse GCs viability by suppressing ER stress markers GRP78 and CHOP [43], but also promoted porcine cumulus cell expansion and oocyte meiotic maturation during *in vitro* maturation by reducing ER stress [44]. In our study, melatonin not only rescued antioxidase expression, inhibited ER stress, delayed GCs senescence and improved fertility in the endometriosis mouse model, but also alleviated 3-NAP-induced OS and increased fertility of mice in the 3-NAP group, although melatonin did not shorten the delay of first birth in endometriosis mice. Together this suggests that the antioxidant protective function of melatonin may be a promising adjuvant therapy to reverse OS-induced fertility decline in endometriosis.

The samples size in our RNA-sequencing was small and more samples are needed for further verification. Though we considered ER stress as a robust cause of GCs senescence in endometriosis, more precise signaling pathways should be explored in the future. In our current study, we just proved that GCs from endometriosis (including early and advanced stage endometriosis) had completely different pathological changes compared with control GCs, a depth comparison of disease stages on GCs function is appreciated in the future. In conclusion, GCs in endometriosis showed most senescent characteristics, such as excessive OS, increased ER stress, and mitochondrial dysfunction-associated reduction of MMP and ATP. Although our results suggest that melatonin may represent a promising strategy for endometriosis adjuvant therapy via alleviating OS-induced GCs senescence, as a versatile compound, melatonin deserves more attention to clarify its role in fecundity improvement of endometriosis and in clinical application. And more research is needed to clarify the mechanisms that underlie GCs senescence in endometriosis.

Funding

This work was supported by grants from National Natural Science Foundation of China (grant numbers 81871135, 81971358, 81671435); National Key Research and Development Program grant

2018YFC1004800; and Key Research and Development Program of Zhejiang Province grant 2017C03022; Clinical Research Special Fund of Chinese Medical Association (18010190748); Medical Science and Technology Project Foundation of Zhejiang Province (2020KY606).

Disclosure summary

The authors have nothing to disclose.

Declaration of competing interest

The authors declare that they have no conflict of interest.

Acknowledgements

Xiang Lin and Yongdong Dai performed experiments. Xiang Lin, Qianmeng Huang, Xiaomei Tong, Feng zhuo and Hanjin Zhou collected the clinical samples. Xiang Lin, Yongdong Dai, Wenzhi Xu and Xiaomei Tong analyzed the data. Xiang Lin and Yongdong Dai made the figures and drafted the article. Yongdong Dai, Xiaoying Jin, Dong Huang and Xiaona Lin critically reviewed the article. Songying Zhang conceived and supervised the project. All authors have read and approved the final version of the paper. We thank Liwen Bianji, Edanz Editing China (www.liwenbianji.cn/ac), for editing the English text of a draft of this manuscript.

Appendix A. Supplementary data

Supplementary data to this article can be found online at https://doi.org/10.1016/j.redox.2020.101431.

References

[1] P. Vercellini, P. Vigano, E. Somigliana, L. Fedele, Endometriosis: pathogenesis and treatment, Nat. Rev. Endocrinol. 10 (5) (2014) 261–275, https://doi.org/10.1038/nrendo.2013.255.

[2] D.A. Dumesic, D.R. Meldrum, M.G. Katz-Jaffe, R.L. Krisher, W.B. Schoolcraft, Oocyte environment: follicular fluid and cumulus cells are critical for oocyte health, Fertil. Steril. 103 (2) (2015) 303–316, https://doi.org/10.1016/j.fertnstert.2014.11.015.

[3] M.G. Da Broi, F.O. de Albuquerque, A.Z. de Andrade, R.L. Cardoso, A.A. Jordao Junior, P.A. Navarro, Increased concentration of 8-hydroxy-2'-deoxyguanosine in follicular fluid of infertile women with endometriosis, Cell Tissue Res. 366 (1) (2016) 231–242, https://doi.org/10.1007/s00441-016-2428-4.

[4] M.G. Da Broi, A.A. Jordao Jr., R.A. Ferriani, P.A. Navarro, Oocyte oxidative DNA damage may be involved in minimal/mild endometriosis-related infertility, Mol. Reprod. Dev. 85 (2) (2018) 128–136, https://doi.org/10.1002/mrd.22943.

[5] D.F. Albertini, C.M. Combelles, E. Benecchi, M.J. Carabatsos, Cellular basis for paracrine regulation of ovarian follicle development, Reproduction 121 (5) (2001) 647–653.

[6] P.A. Perez-Mancera, A.R. Young, M. Narita, Inside and out: the activities of senescence in cancer, Nat. Rev. Cancer 14 (8) (2014) 547–558, https://doi.org/10.1038/nrc3773.

[7] Y. Sun, J.P. Coppe, E.W. Lam, Cellular senescence: the sought or the unwanted? Trends Mol. Med. 24 (10) (2018) 871–885, https://doi.org/10.1016/j.molmed.2018.08.002.

[8] A. Guillaumet-Adkins, Y. Yanez, M.D. Peris-Diaz, I. Calabria, C. Palanca-Ballester, J. Sandoval, Epigenetics and oxidative stress in aging, Oxid. Med. Cell Longev. 2017 (2017) 9175806, https://doi.org/10.1155/2017/9175806.

[9] A. Hohn, D. Weber, T. Jung, C. Ott, M. Hugo, B. Kochlik, ... J.P. Castro, Happily (n) ever after: aging in the context of oxidative stress, proteostasis loss and cellular senescence, Redox Biol. 11 (2017) 482–501, https://doi.org/10.1016/j.redox.2016.12.001.

[10] Z. Zhang, L. Zhang, L. Zhou, Y. Lei, Y. Zhang, C. Huang, Redox signaling and unfolded protein response coordinate cell fate decisions under ER stress, Redox Biol. (2018), https://doi.org/10.1016/j.redox.2018.11.005.

[11] Y.S. Lee, D.H. Lee, H.A. Choudry, D.L. Bartlett, Y.J. Lee, Ferroptosis-induced endoplasmic reticulum stress: cross-talk between ferroptosis and apoptosis, Mol. Cancer Res. 16 (7) (2018) 1073–1076, https://doi.org/10.1158/1541-7786.MCR-18-0055.

[12] O. Pluquet, A. Pourtier, C. Abbadie, The unfolded protein response and cellular senescence. A review in the theme: cellular mechanisms of endoplasmic reticulum stress signaling in health and disease, Am. J. Physiol. Cell Physiol. 308 (6) (2015) C415–C425, https://doi.org/10.1152/ajpcell.00334.2014.

[13] J.J. Tarin, Aetiology of age-associated aneuploidy: a mechanism based on the 'free radical theory of ageing, Hum. Reprod. 10 (6) (1995) 1563–1565, https://doi.org/10.1093/humrep/10.6.1563.

[14] J. Qiao, Z.B. Wang, H.L. Feng, Y.L. Miao, Q. Wang, Y. Yu, ... Q.Y. Sun, The root of reduced fertility in aged women and possible therapentic options: current status and future perspects, Mol. Asp. Med. 38 (2014) 54–85, https://doi.org/10.1016/j.mam.2013.06.001.

[15] J.P. Coppe, C.K. Patil, F. Rodier, Y. Sun, D.P. Munoz, J. Goldstein, ... J. Campisi, Senescence-associated secretory phenotypes reveal cell-nonautonomous functions of oncogenic RAS and the p53 tumor suppressor, PLoS Biol. 6 (12) (2008) 2853–2868, https://doi.org/10.1371/journal.pbio.0060301.

[16] S. He, N.E. Sharpless, Senescence in health and disease, Cell 169 (6) (2017) 1000–1011, https://doi.org/10.1016/j.cell.2017.05.015.

[17] T. Ito, Y.V. Teo, S.A. Evans, N. Neretti, J.M. Sedivy, Regulation of cellular senescence by polycomb chromatin modifiers through distinct DNA damage- and histone methylation-dependent pathways, Cell Rep. 22 (13) (2018) 3480–3492, https://doi.org/10.1016/j.celrep.2018.03.002.

[18] Y. Liu, M. Han, X. Li, H. Wang, M. Ma, S. Zhang, ... Y. Yao, Age-related changes in the mitochondria of human mural granulosa cells, Hum. Reprod. 32 (12) (2017) 2465–2473, https://doi.org/10.1093/humrep/dex309.

[19] Y. Dai, X. Lin, W. Xu, X. Lin, Q. Huang, L. Shi, ... S. Zhang, MiR-210-3p protects endometriotic cells from oxidative stress-induced cell cycle arrest by targeting BARD1, Cell Death Dis. 10 (2) (2019) 144, https://doi.org/10.1038/s41419-019-1395-6.

[20] A. Chandrasekaran, M. Idelchik, J.A. Melendez, Redox control of senescence and age-related disease, Redox Biol. 11 (2017) 91–102, https://doi.org/10.1016/j.redox.2016.11.005.

[21] D.V. Ziegler, C.D. Wiley, M.C. Velarde, Mitochondrial effectors of cellular senescence: beyond the free radical theory of aging, Aging Cell 14 (1) (2015) 1–7, https://doi.org/10.1111/acel.12287.

[22] A. Calcinotto, J. Kohli, E. Zagato, L. Pellegrini, M. Demaria, A. Alimonti, Cellular senescence: aging, cancer, and injury, Physiol. Rev. 99 (2) (2019) 1047–1078, https://doi.org/10.1152/physrev.00020.2018.

[23] E.Y. Fujii, M. Nakayama, The measurements of RAGE, VEGF, and AGEs in the plasma and follicular fluid of reproductive women: the influence of aging, Fertil. Steril. 94 (2) (2010) 694–700, https://doi.org/10.1016/j.fertnstert.2009.03.029.

[24] Z. Merhi, M. Irani, A.D. Doswell, J. Ambroggio, Follicular fluid soluble receptor for advanced glycation end-products (sRAGE): a potential indicator of ovarian reserve, J. Clin. Endocrinol. Metab. 99 (2) (2014) E226–E233, https://doi.org/10.1210/jc.2013-3839.

[25] S. Ressler, J. Bartkova, H. Niederegger, J. Bartek, K. Scharffetter-Kochanek, P. Jansen-Durr, M. Wlaschek, p16INK4A is a robust in vivo biomarker of cellular aging in human skin, Aging Cell 5 (5) (2006) 379–389, https://doi.org/10.1111/j.1474-9726.2006.00231.x.

[26] E. Bertero, C. Maack, Calcium signaling and reactive oxygen species in mitochondria, Circ. Res. 122 (10) (2018) 1460–1478, https://doi.org/10.1161/CIRCRESAHA.118.310082.

[27] E. Guzel, S. Arlier, O. Guzeloglu-Kayisli, M.S. Tabak, T. Ekiz, N. Semerci, ... U.A. Kayisli, Endoplasmic reticulum stress and homeostasis in reproductive physiology and pathology, Int. J. Mol. Sci. 18 (4) (2017), https://doi.org/10.3390/ijms18040792.

[28] G. Martinez, C. Duran-Aniotz, F. Cabral-Miranda, J.P. Vivar, C. Hetz, Endoplasmic reticulum proteostasis impairment in aging, Aging Cell 16 (4) (2017) 615–623, https://doi.org/10.1111/acel.12599.

[29] N. Takahashi, M. Harada, Y. Hirota, E. Nose, J.M. Azhary, H. Koike, ... Y. Osuga, Activation of endoplasmic reticulum stress in granulosa cells from patients with polycystic ovary syndrome contributes to ovarian fibrosis, Sci. Rep. 7 (1) (2017) 10824, https://doi.org/10.1038/s41598-017-11252-7.

[30] H. Tamura, M. Kawamoto, S. Sato, I. Tamura, R. Maekawa, T. Taketani, ... N. Sugino, Long-term melatonin treatment delays ovarian aging, J. Pineal Res. 62 (2) (2017), https://doi.org/10.1111/jpi.12381.

[31] G.W. Kim, P.H. Chan, Oxidative stress and neuronal DNA fragmentation mediate age-dependent vulnerability to the mitochondrial toxin, 3-nitropropionic acid, in the mouse striatum, Neurobiol. Dis. 8 (1) (2001) 114–126, https://doi.org/10.1006/nbdi.2000.0327.

[32] M. Shen, F. Lin, J. Zhang, Y. Tang, W.K. Chen, H. Liu, Involvement of the up-regulated FoxO1 expression in follicular granulosa cell apoptosis induced by oxidative stress, J. Biol. Chem. 287 (31) (2012) 25727–25740, https://doi.org/10.1074/jbc.M112.349902.

[33] A.M. Sanchez, P. Vigano, F. Quattrone, L. Pagliardini, E. Papaleo, M. Candiani, P. Panina-Bordignon, The WNT/beta-catenin signaling pathway and expression of survival promoting genes in luteinized granulosa cells: endometriosis as a paradigm for a dysregulated apoptosis pathway, Fertil. Steril. 101 (6) (2014) 1688–1696, https://doi.org/10.1016/j.fertnstert.2014.02.040.

[34] N. Takahashi, M. Harada, J.M.K. Azhary, C. Kunitomi, E. Nose, H. Terao, ... Y. Osuga, Accumulation of advanced glycation end products in follicles is associated with poor oocyte developmental competence, Mol. Hum. Reprod. (2019), https://doi.org/10.1093/molehr/gaz050.

[35] D.K. Hapangama, A. Kamal, G. Saretzki, Implications of telomeres and telomerase in endometrial pathology, Hum. Reprod. Update 23 (2) (2017) 166–187, https://doi.org/10.1093/humupd/dmw044.

[36] R.C. Dracxler, C. Oh, K. Kalmbach, F. Wang, L. Liu, E.G. Kallas, ... M.S. Abrao, Peripheral blood telomere content is greater in patients with endometriosis than in controls, Reprod. Sci. 21 (12) (2014) 1465–1471, https://doi.org/10.1177/1933719114527353.

[37] C. Tatone, M.C. Carbone, S. Falone, P. Aimola, A. Giardinelli, D. Caserta, ... F. Amicarelli, Age-dependent changes in the expression of superoxide dismutases

and catalase are associated with ultrastructural modifications in human granulosa cells, Mol. Hum. Reprod. 12 (11) (2006) 655–660, https://doi.org/10.1093/molehr/gal080.

[38] X. Yang, L.L. Wu, L.R. Chura, X. Liang, M. Lane, R.J. Norman, R.L. Robker, Exposure to lipid-rich follicular fluid is associated with endoplasmic reticulum stress and impaired oocyte maturation in cumulus-oocyte complexes, Fertil. Steril. 97 (6) (2012) 1438–1443, https://doi.org/10.1016/j.fertnstert.2012.02.034.

[39] Y. Zeng, H. Sun, Y. Li, M. Shao, P. Han, X. Yu, ... S. Li, Exposure to triptolide affects follicle development in NIH mice: role of endoplasmic reticulum stress in granulosa cell apoptosis, Hum. Exp. Toxicol. 36 (1) (2017) 82–92, https://doi.org/10.1177/0960327116638725.

[40] R.J. Reiter, J.C. Mayo, D.X. Tan, R.M. Sainz, M. Alatorre-Jimenez, L. Qin, Melatonin as an antioxidant: under promises but over delivers, J. Pineal Res. 61 (3) (2016) 253–278, https://doi.org/10.1111/jpi.12360.

[41] G. Paradies, V. Paradies, F.M. Ruggiero, G. Petrosillo, Mitochondrial bioenergetics decay in aging: beneficial effect of melatonin, Cell. Mol. Life Sci. 74 (21) (2017) 3897–3911, https://doi.org/10.1007/s00018-017-2619-5.

[42] C. Song, W. Peng, S. Yin, J. Zhao, B. Fu, J. Zhang, ... Y. Zhang, Melatonin improves age-induced fertility decline and attenuates ovarian mitochondrial oxidative stress in mice, Sci. Rep. 6 (2016) 35165, https://doi.org/10.1038/srep35165.

[43] Z. Chen, L. Lei, D. Wen, L. Yang, Melatonin attenuates palmitic acid-induced mouse granulosa cells apoptosis via endoplasmic reticulum stress, J. Ovarian Res. 12 (1) (2019) 43, https://doi.org/10.1186/s13048-019-0519-z.

[44] H.J. Park, J.Y. Park, J.W. Kim, S.G. Yang, J.M. Jung, M.J. Kim, ... D.B. Koo, Melatonin improves the meiotic maturation of porcine oocytes by reducing endoplasmic reticulum stress during in vitro maturation, J. Pineal Res. 64 (2) (2018), https://doi.org/10.1111/jpi.12458.